

# Non-axisymmetric fields, Plasma Rotation, and Locked Modes on Alcator C-Mod



I.H.Hutchinson, S.M.Wolfe,  
R.S.Granetz, J.Rice, A.Hubbard, J.Irby  
Plasma Science and Fusion Center,  
MIT, Cambridge, MA, USA

# A new initiative on C-Mod



For its first 9 years of operation we paid little attention to error fields and locked modes on C-Mod. Although rotation has been a major topic.

- Locked modes rarely seemed to be a problem.
- Most plasmas were fairly high density.
- Locked modes were rather hard to detect.
- Scaling from other machines indicated a small machine like C-Mod should not have locked modes.

During 2001-2 Locked modes began to be unequivocally detected and an operational annoyance especially:

- In long-pulse operation at low density.
- During higher plasma current operation.

Last APS I had many helpful discussions with DIIID colleagues and decided

- We should get serious about field asymmetries (error fields).
- Best way to do this was to install coils (A-coils) to apply them.

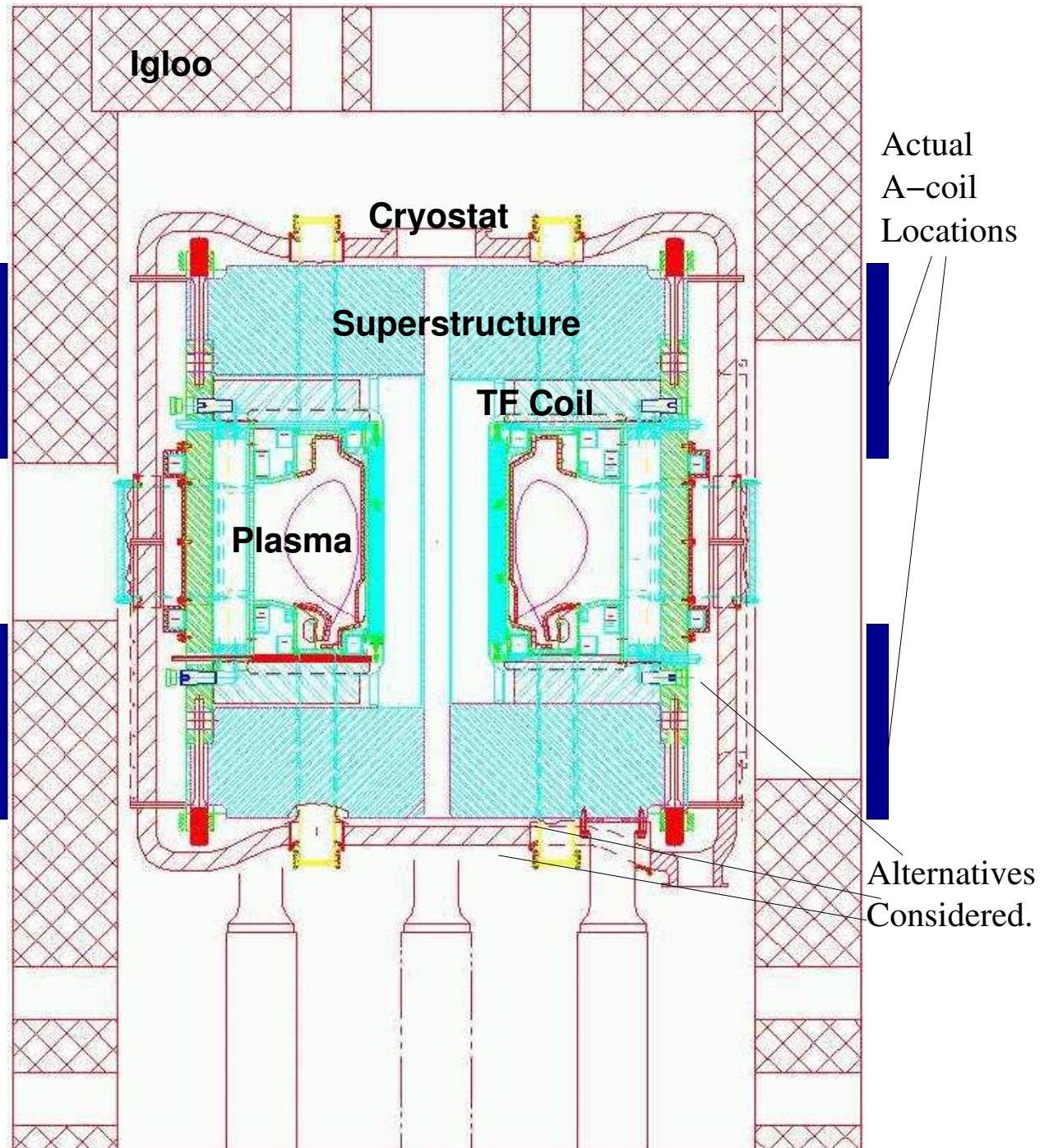
# Retrofitted Asymmetric Coils Compromise

We had access to the tokamak superstructure.

Considered several positions closer to the plasma, inside or outside of the cryostat.

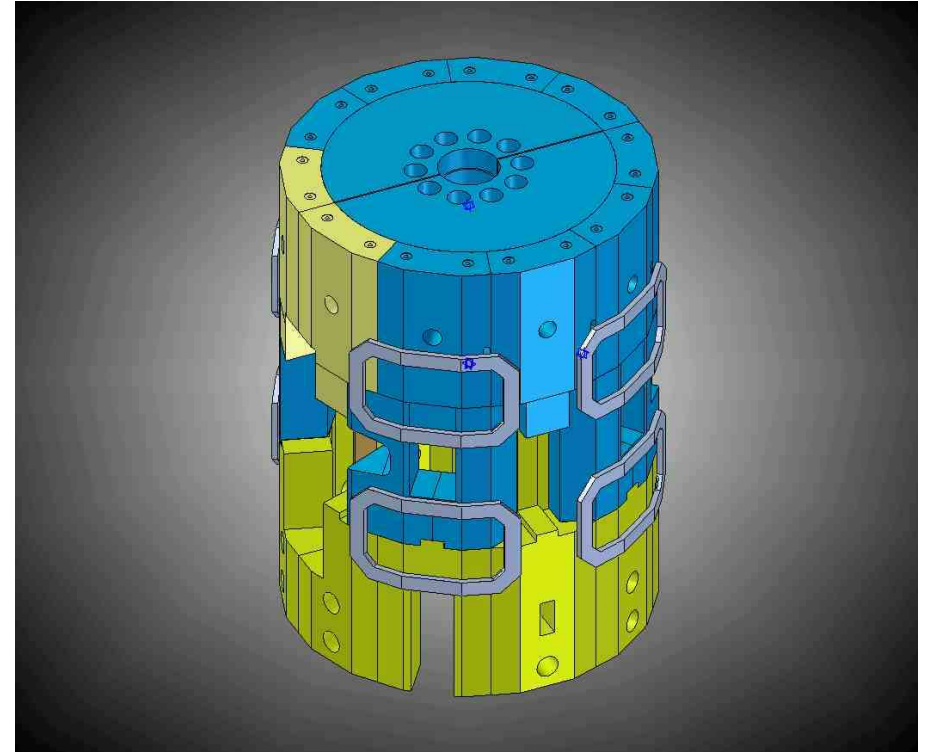
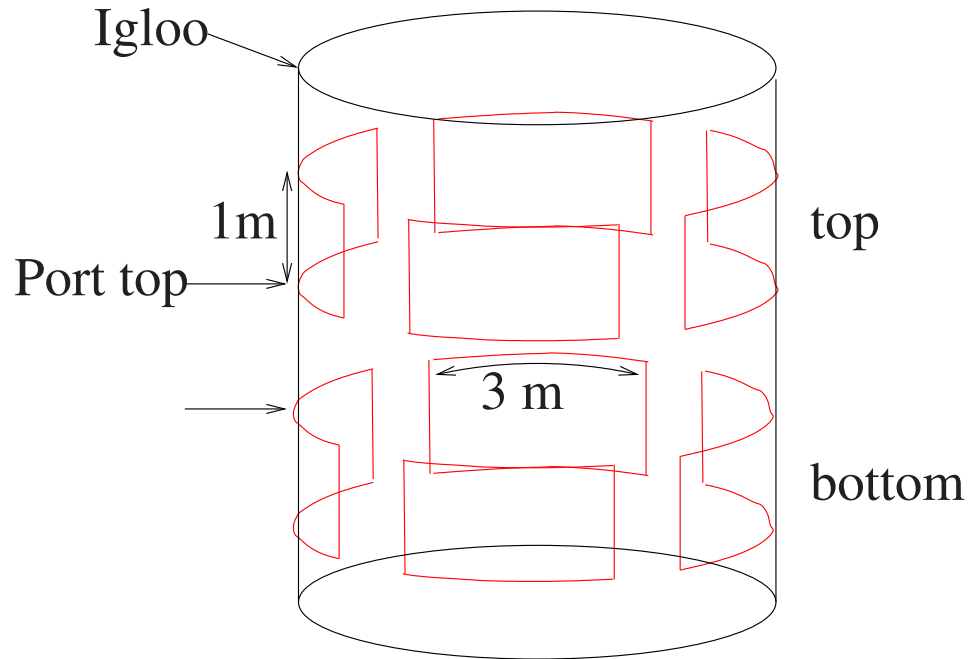
Eventually settled on coils further from the plasma as the most practical short-term solution.

They are far from the plasma, which influences the m-spectrum.



# C-Mod's New Asymmetric Coil set

For applying controlled field perturbations



- Coils: 27 turns to  $> 3$  kA/turn.
- Each coil separately controlled. Choose any subset in series/parallel.
- Allows a wide range of phase/helicity of perturbation.
- Enables relative size of (2,1) and (1,1) to be varied.
- Installed simply and quickly in accessible location.
- One coil omitted initially because of mechanical interference.

# Simple Coil Design, Manufactured In-House



Coils operational during entire 2003 campaign.

Driven in series (or parallel) by single programmable 3kA supply.

Fringing field effect on equipment must be considered.



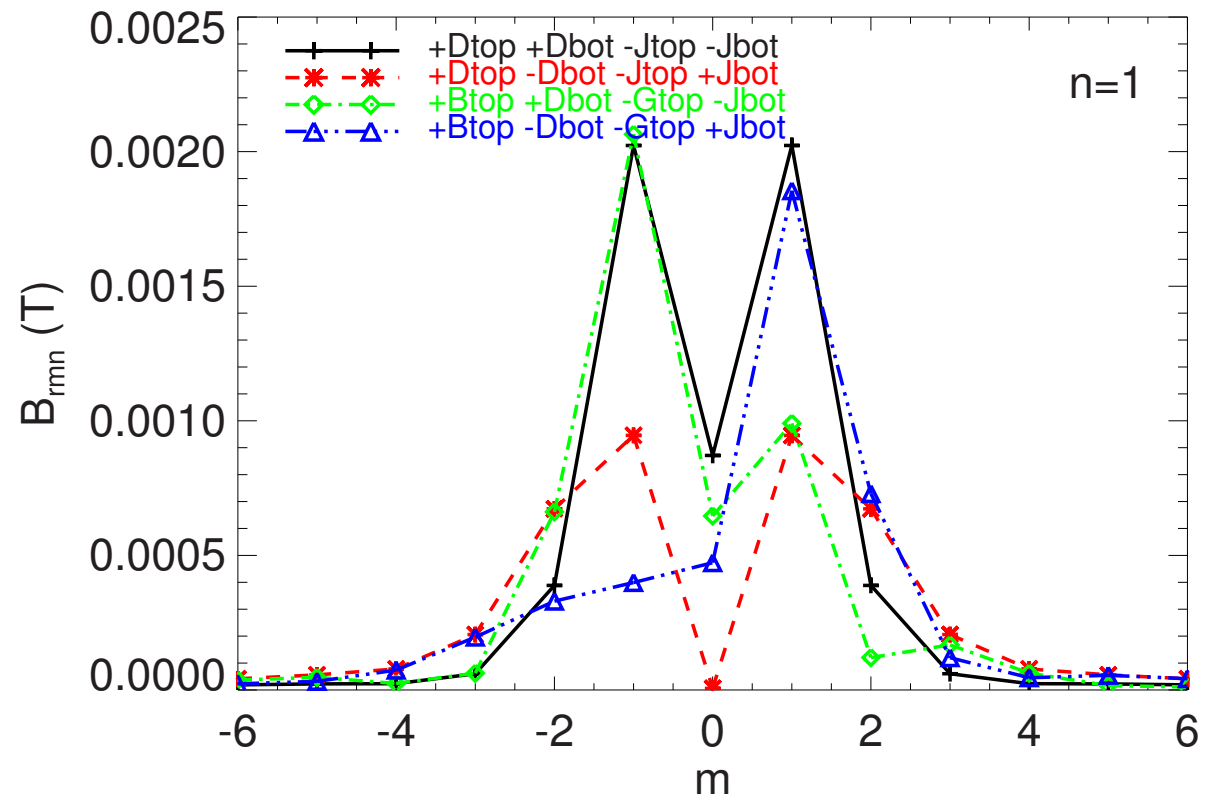
# Perturbation mode spectra at q=2 surface, mostly m=1,2

$$B_{mn} = \frac{1}{2\pi^2} \int_0^{2\pi} d\phi \int_0^{2\pi} d\hat{\theta} B_{\perp}(\phi, \hat{\theta}) e^{-j(n\phi+m\hat{\theta})}, \quad \hat{\theta} \equiv \frac{1}{q} \int dl \frac{B_{\phi}}{RB_p}.$$

Examples of mode spectra for different coil combinations.

Can obtain amplitude (1, 1) ~ (2, 1) but more typically the (1,1) component is larger.

m=3 component is always much smaller than m=2.



Handedness of perturbation can be reversed. (Compare green and blue).

We expect that reversed helicity, non-resonant fields produce no observable effects.

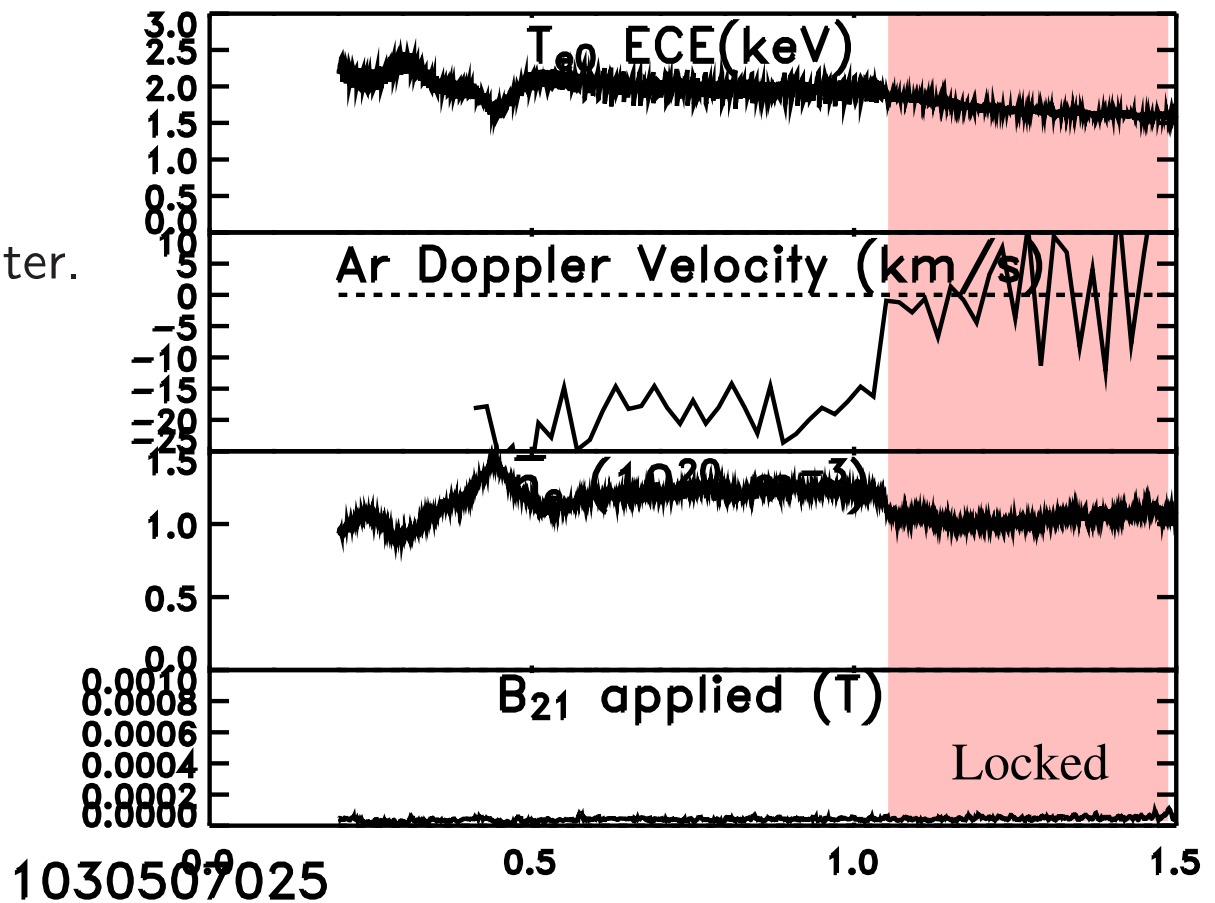
# Mode locking slows previously rotating plasma core velocity to zero

Sawtooth size reduction characteristic symptom of locking

Toroidal velocity, negative  $\equiv$  counter. Slows to zero on locking.

Locking density quite high for this ohmic 1MA plasma.

No applied asymmetric field. Intrinsic error only.



Symptoms of locking are often not as clear as this.

Magnetic diagnostics are rarely definitive at low current, c.f. noise levels.

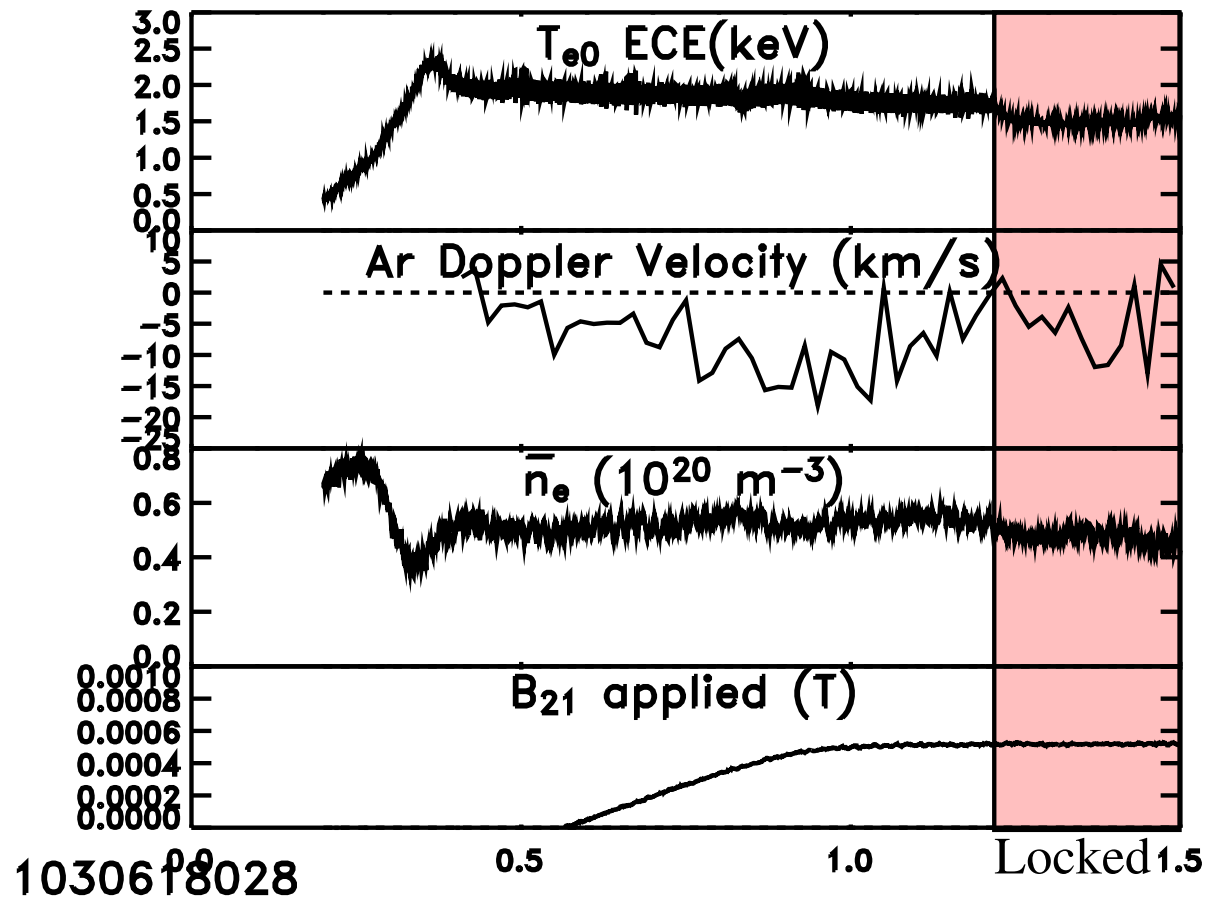
# Locking sometimes seems to take time

$I_p = 0.6\text{MA}$ ,  $B_t = 4$ ,  $q = 5$ .

Locking occurs about 200ms after reaching full applied field.

The intrinsic error field may be changing in time.

Or there may be other subtle variations of the important parameters like rotation.



# Coil Options Selected by Patch Panel

Allow shot-to-shot variation of applied phase

Patch Panel  
in cell close to  
tokamak.

Configuration  
change takes  
~ 10 minutes.



Also permits variation of the m-spectrum and helicity.

# Different A-coil Connections allow many Different (2,1) Phases

	Bt	Bb	Dt	Db	Gt	Gb	Jt	Jb	(1,1)T/A	(2,1)T/A	Phase	B <sub>21</sub> mT
A	0	0	1	-1	0	0	-1	1	4.11e-07	2.93e-07	0.3957	0.6649
B	0	0	1	1	0	0	-1	-1	8.80e-07	1.69e-07	2.0230	0.3839
C	-1	0	0	1	1	0	0	-1	8.06e-07	3.17e-07	2.8963	0.7209
D	0	0	1	0	0	-1	-1	0	7.12e-07	2.32e-07	1.2144	0.6950
E	0	0	1	0	0	0	-1	1	3.70e-07	2.21e-07	0.5875	0.6633
F	0	0	1	-1	0	-1	-1	0	6.15e-07	2.66e-07	0.8934	0.6047
G	0	0	1	-1	-1	0	0	0	4.43e-07	2.15e-07	0.1408	0.6456
H	0	0	1	0	1	-1	0	0	4.16e-07	1.83e-07	1.8265	0.5492
I	-1	0	0	0	1	-1	0	0	3.30e-07	2.09e-07	2.3929	0.6267
J	1	0	1	-1	0	0	0	0	3.83e-07	1.94e-07	0.1297	0.5830
K	-1	0	1	0	1	0	0	-1	6.55e-07	2.18e-07	2.4839	0.4960
L	1	0	0	0	-1	-1	0	0	6.00e-07	1.22e-07	0.2265	0.3650
M	0	0	1	-1	0	0	-1	0	3.70e-07	2.21e-07	0.5875	0.6633

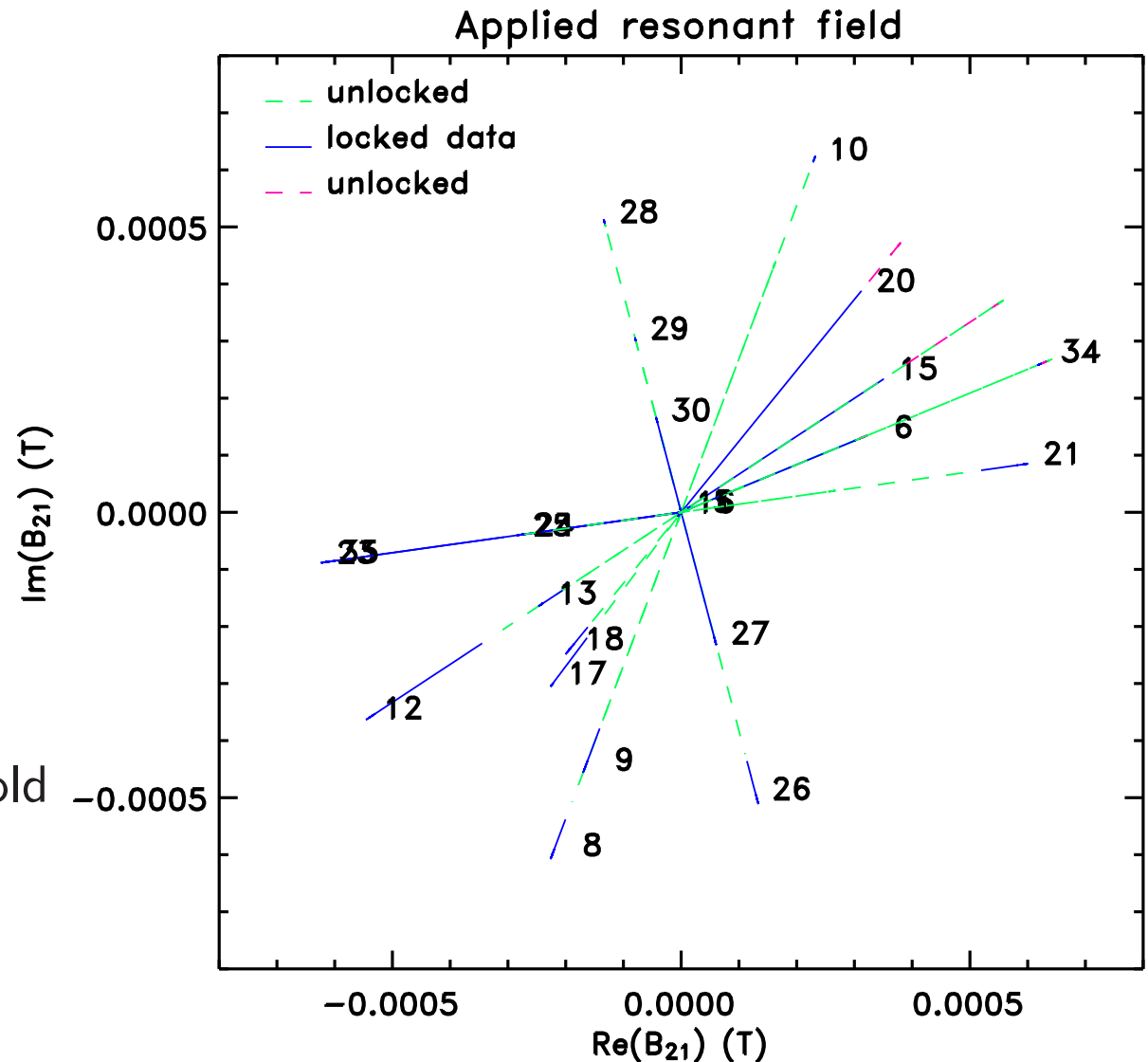
# Mode field represented as a Complex Quantity Enables Phase Comparison

Applied field ramps from (0,0) to a maximum along a radial path as time passes.

Some shots start locked. Such shots unlock (red) later when applied field is in first quadrant ( $x, y > 0$ ).

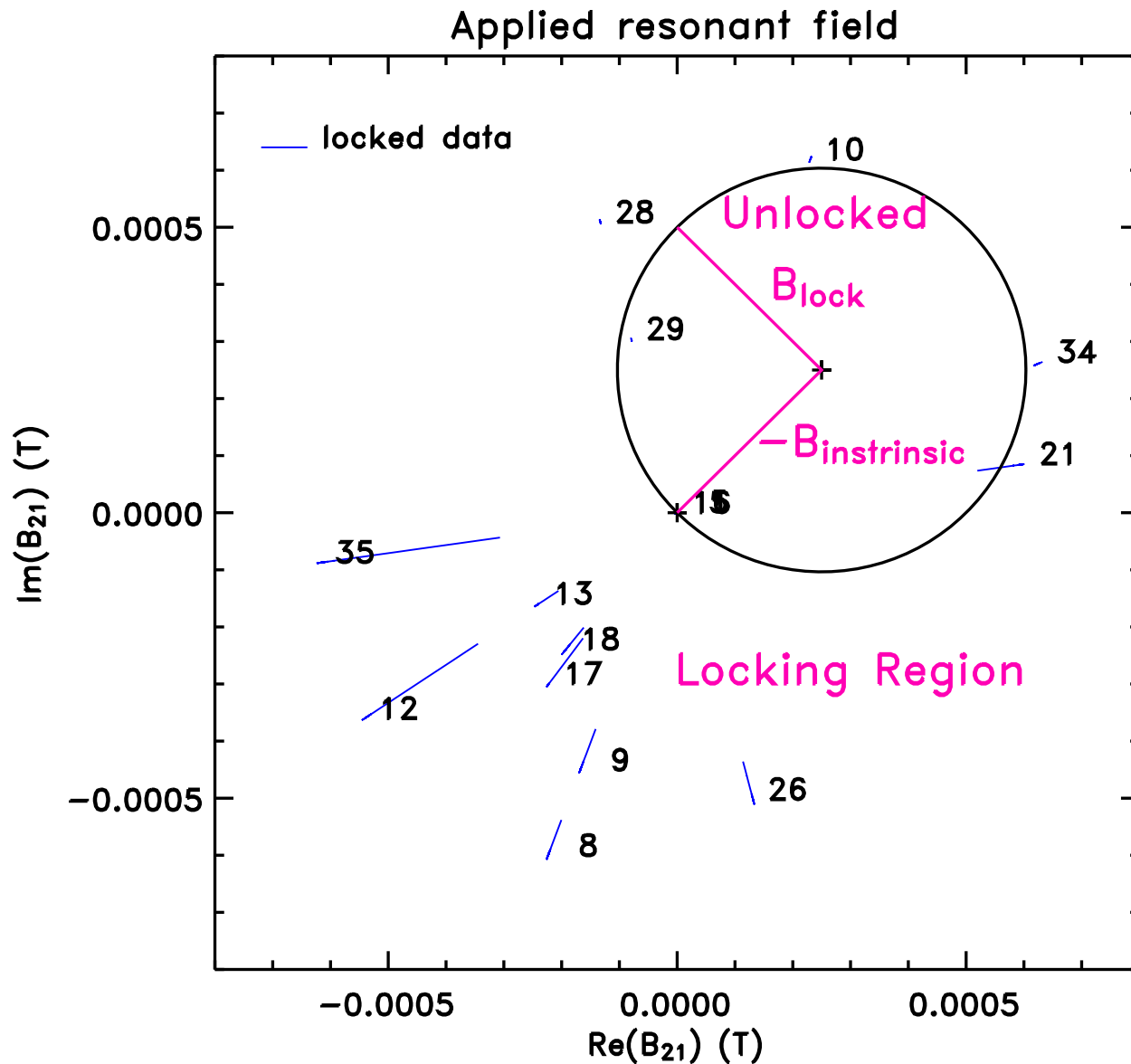
All shots in quadrants 2-4 eventually lock (at these near-threshold conditions).

Other data indicates open regions of quadrants 2,4 are not stabilizing.



Moderate  $B_{21}$  in quadrant 1 suppresses locking.

# Interpretation of Mode Locking at 0.6 MA



Exclude data from shots that started locked.

Fit a circle in the unlocked, i.e. suppression region.

Locking occurs when

$$|B_{21} + B_{intrinsic}| \gtrsim |B_{lock}|$$

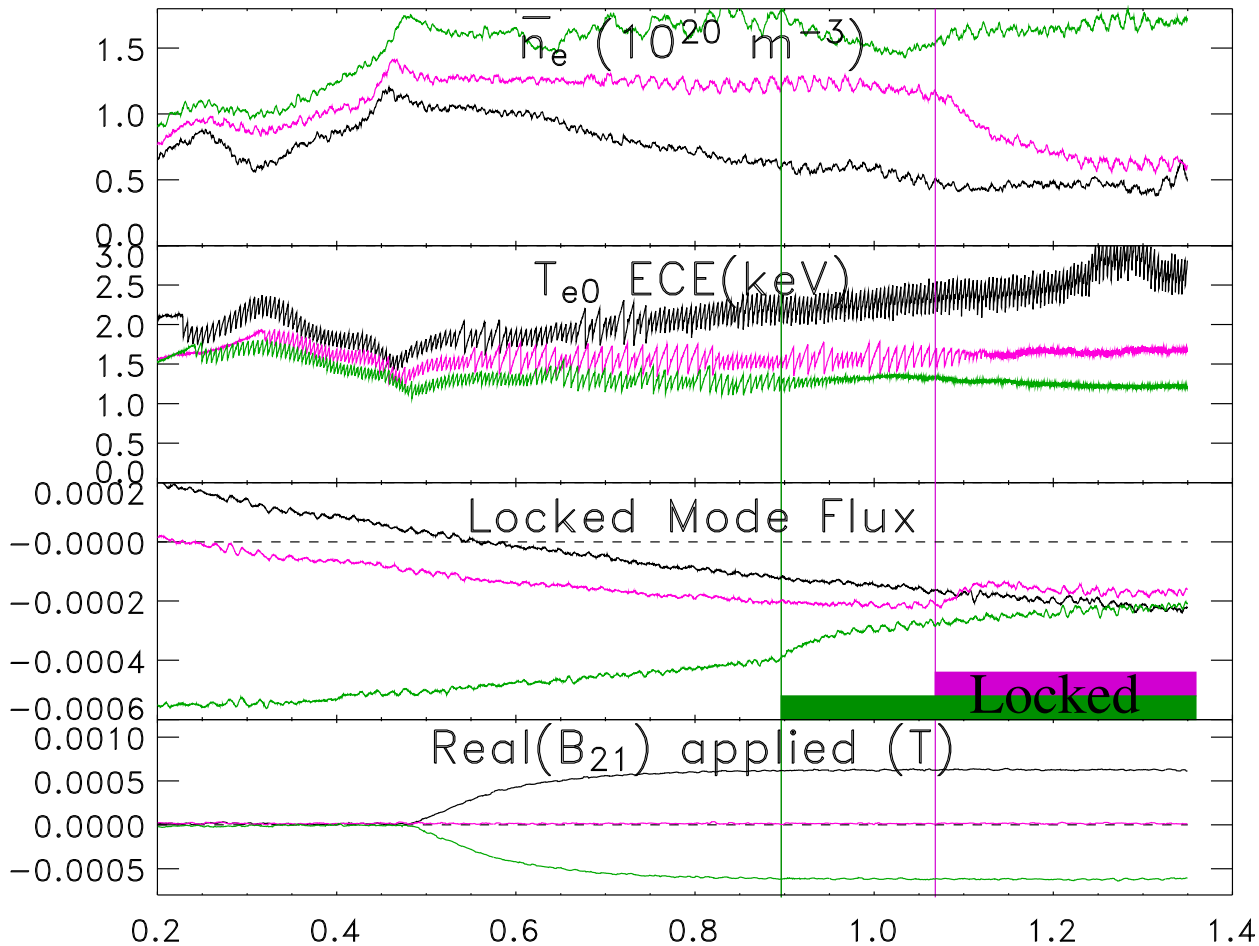
that is, outside the circle.

The center and radius of the circle are deduced from the observations.

We deduce  $-B_{intrinsic} \approx 0.25 + 0.25i$  mT

and  $B_{lock} \approx 0.35$  mT at this density ( $\sim 5 \times 10^{19} \text{ m}^{-3}$ ).

# Correction Allows Very Low Density



Density at lock reduced from  $n_e/10^{20} = 1.7$  for adverse applied field (green), 1.1 for intrinsic field (red),  $< 0.4$  for “best” (black).

These 1MA, 5.4T plasmas have visible mode penetration on flux monitors (whose baseline wanders).

A factor of at least 4 reduction of locking density shows we are compensating the intrinsic error very well in “best” case.

This serves to identify (minus) the intrinsic error for these 1MA plasmas.

# Comparison with Prior Scalings

LaHaye 1997 strong size scaling is contradicted by C-Mod

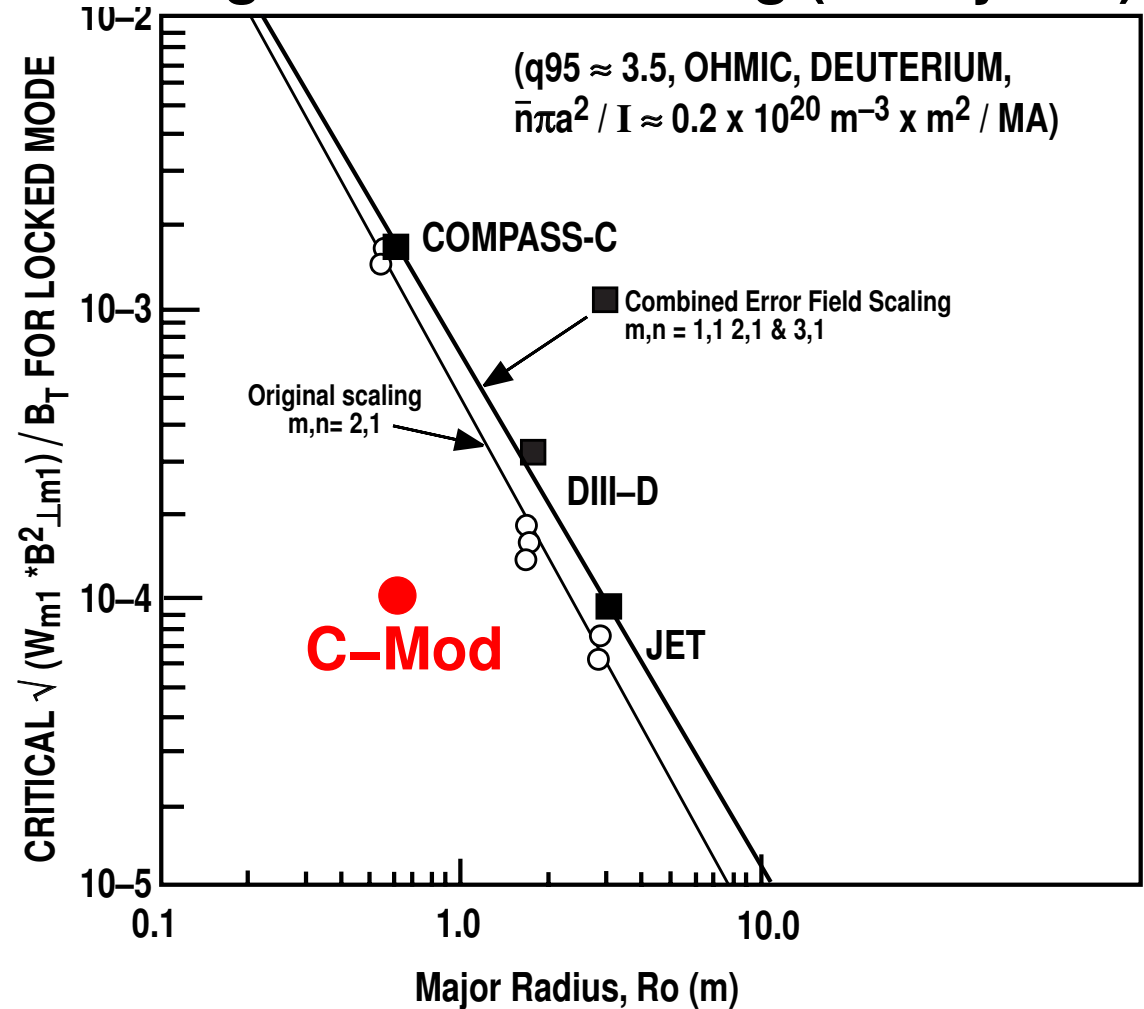
Scaling developed by comparing Compass/DIII-D/JET data.

Experimental scaling of threshold with size appeared very bad for ITER.

Supported by theory-based arguments for  $B_{\text{lock}} \propto R^{-9/5}$

C-Mod locking threshold is factor  $> 10$  below scaling,  $\sim$  same fractional value as for DIII-D and JET.

## Locking Threshold Scaling (LaHaye 97)



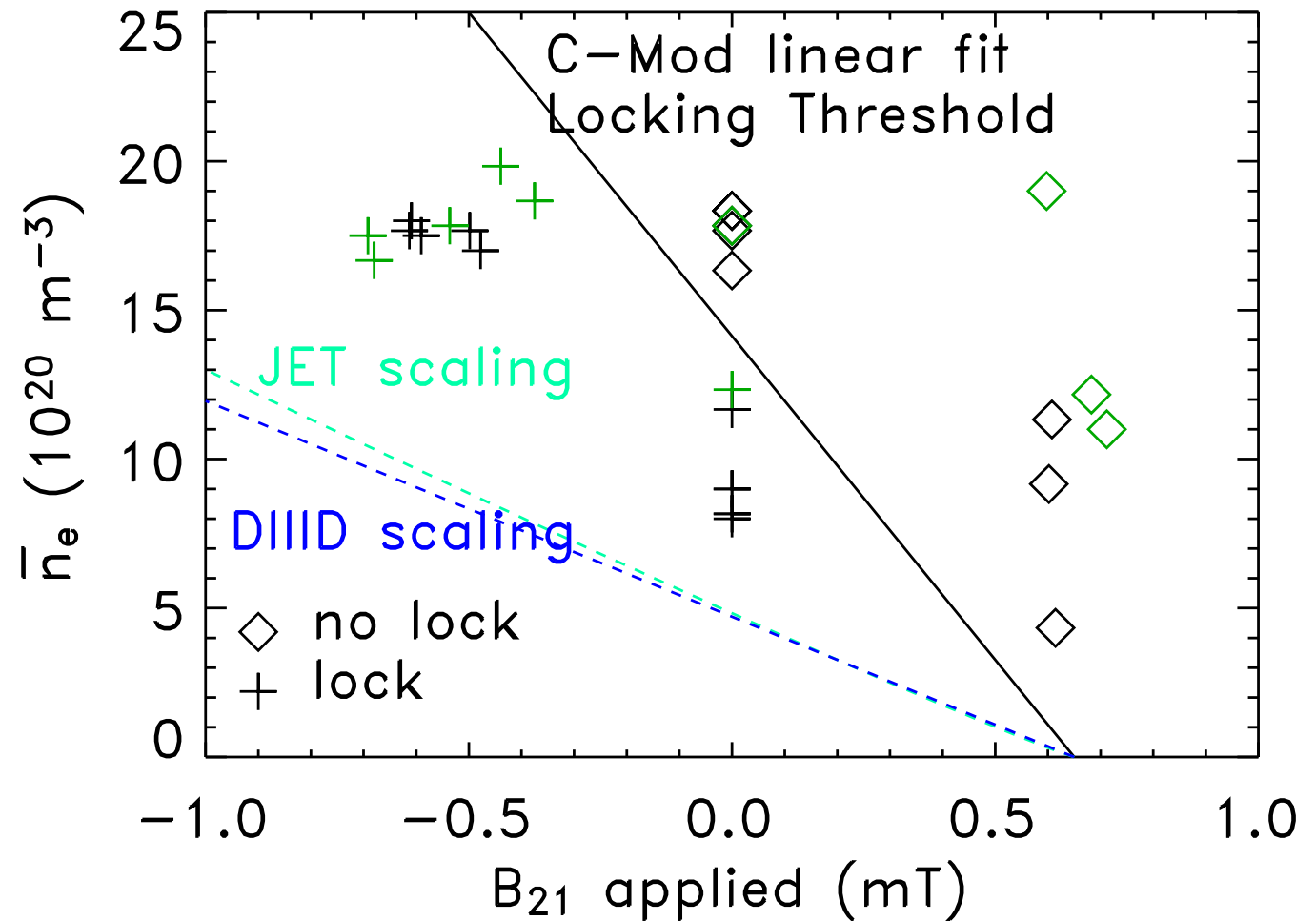
[Compass data different from others, has very strong inverse  $B_t$  scaling.]

# C-Mod locks at higher density than predicted by Prior Scalings

Scaling based on dimensionless analysis and the observed  $n$  and  $B$  dependence [1] developed from single-machine data. ( $B_{\text{lock}}/B_t \propto n^{\alpha_n} B^{\alpha_B} R^{2\alpha_n+1.25\alpha_B}$ )

1MA, 5.4T,  $q_{95} = 3.9$   
locking map enables the C-Mod threshold density to be determined.

It is about  $2\times$  scalings based on JET and DIII-D fits.



[1] R.Buttery et al, Nuclear Fusion 39, 1827 (1999).

# Understanding the Intrinsic Field Error

On Alcator C-Mod



We have not made specific, high-precision field measurements, beyond the standard diagnostic coils.

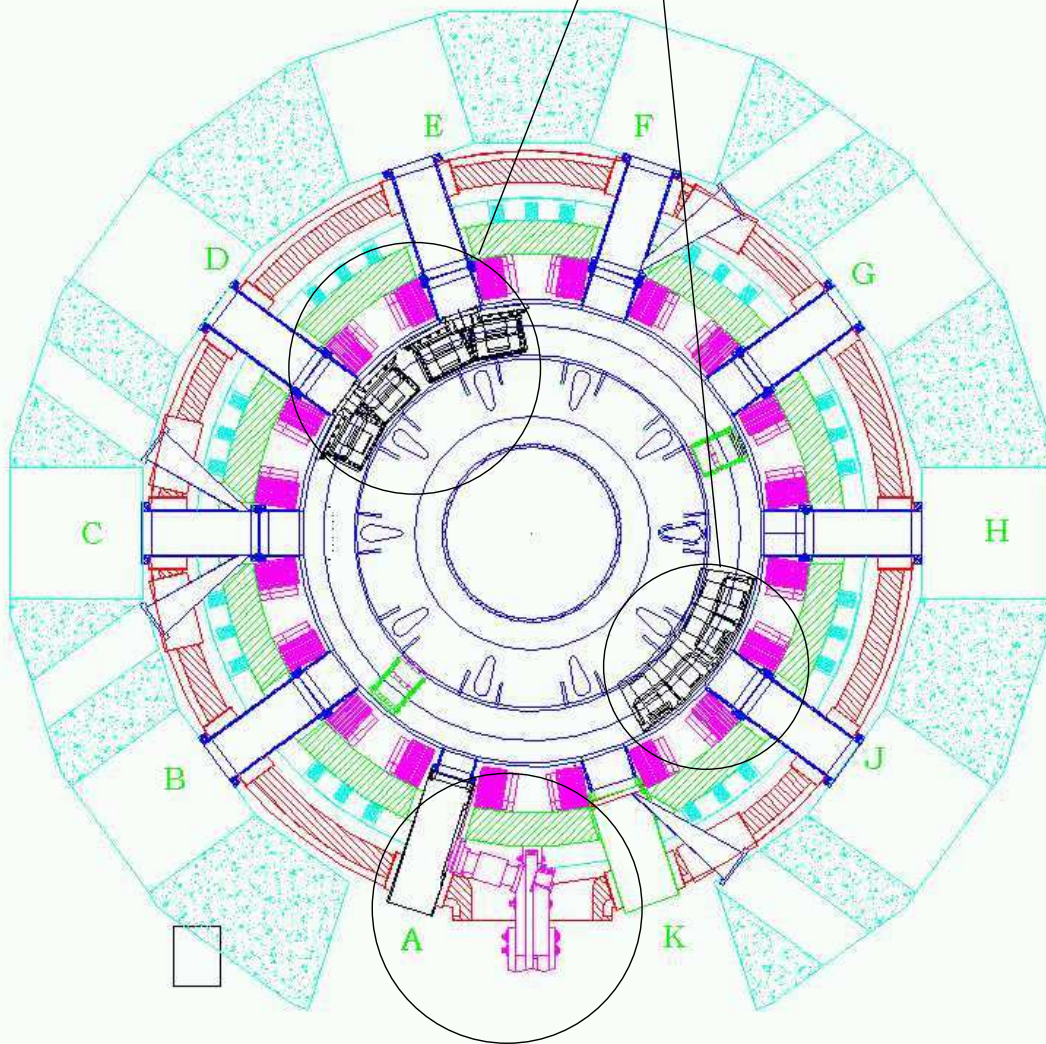
It would be extremely hard for us to do so, because during manned access to the vacuum vessel coils cannot be at liquid nitrogen temperature.

Instead we have

- done a thorough survey of known error sources
- done measurements using existing diagnostics and
- done careful fitting of individual coil contributions

# Known Sources of Asymmetry

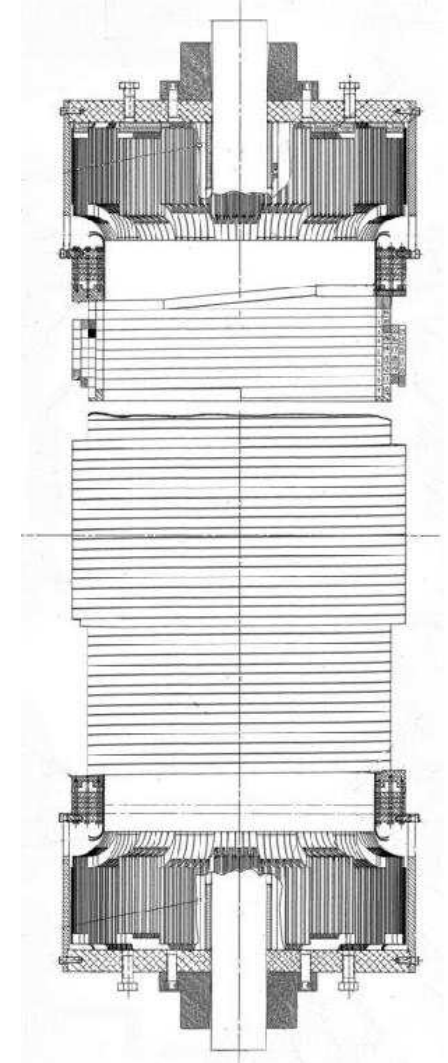
## Asymmetric vessel structures



## TF Bus Connection

TF bus/feed and OH1 winding are the dominant identified sources.  
Asymmetric structures and PF feeds are calculated negligible.

## OH winding turn transitions

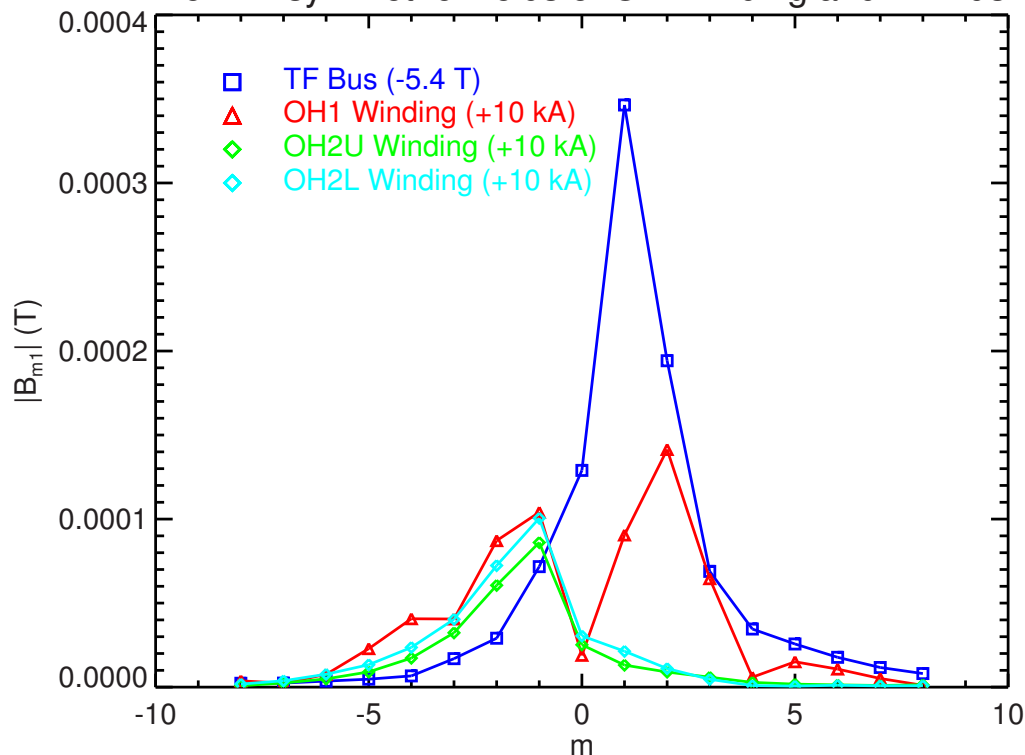


# Mode Structure of TF and OH asymmetries

Strong  $m = 1, 2$  contributions, in quadrant 3

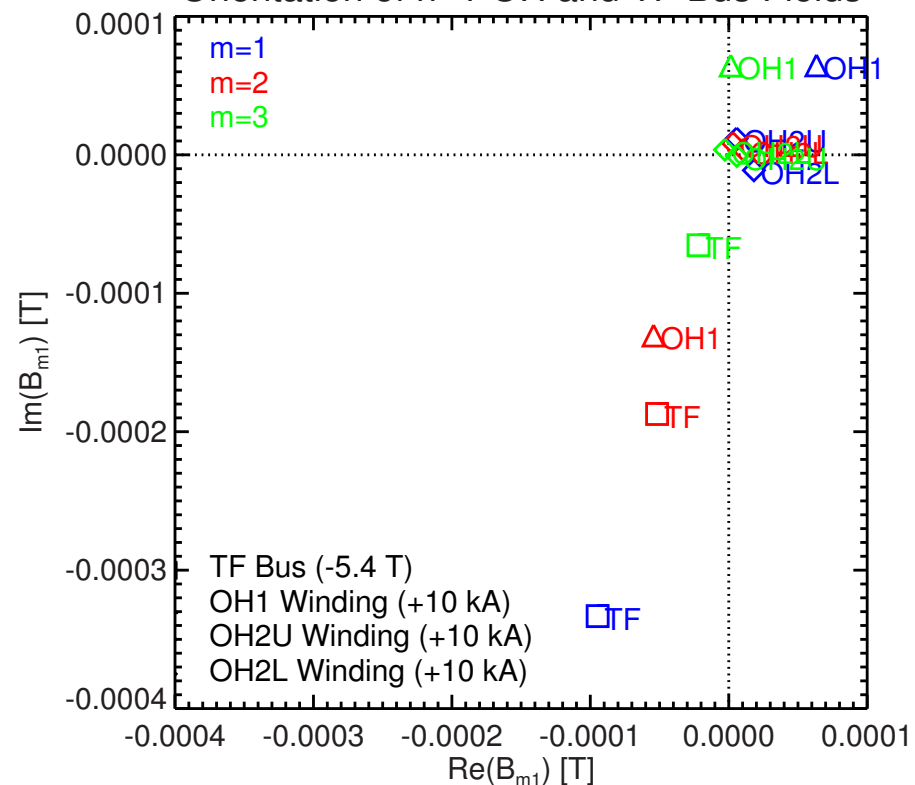
### Mode Poloidal Spectra

Non-Axisymmetric Fields of OH Winding and TF Bus



### Complex Amplitudes

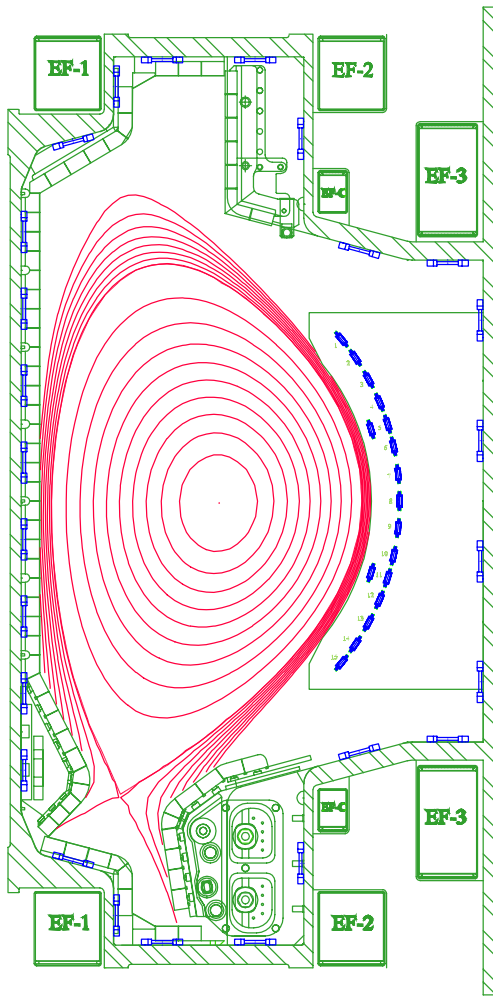
Orientation of  $n=1$  OH and TF Bus Fields



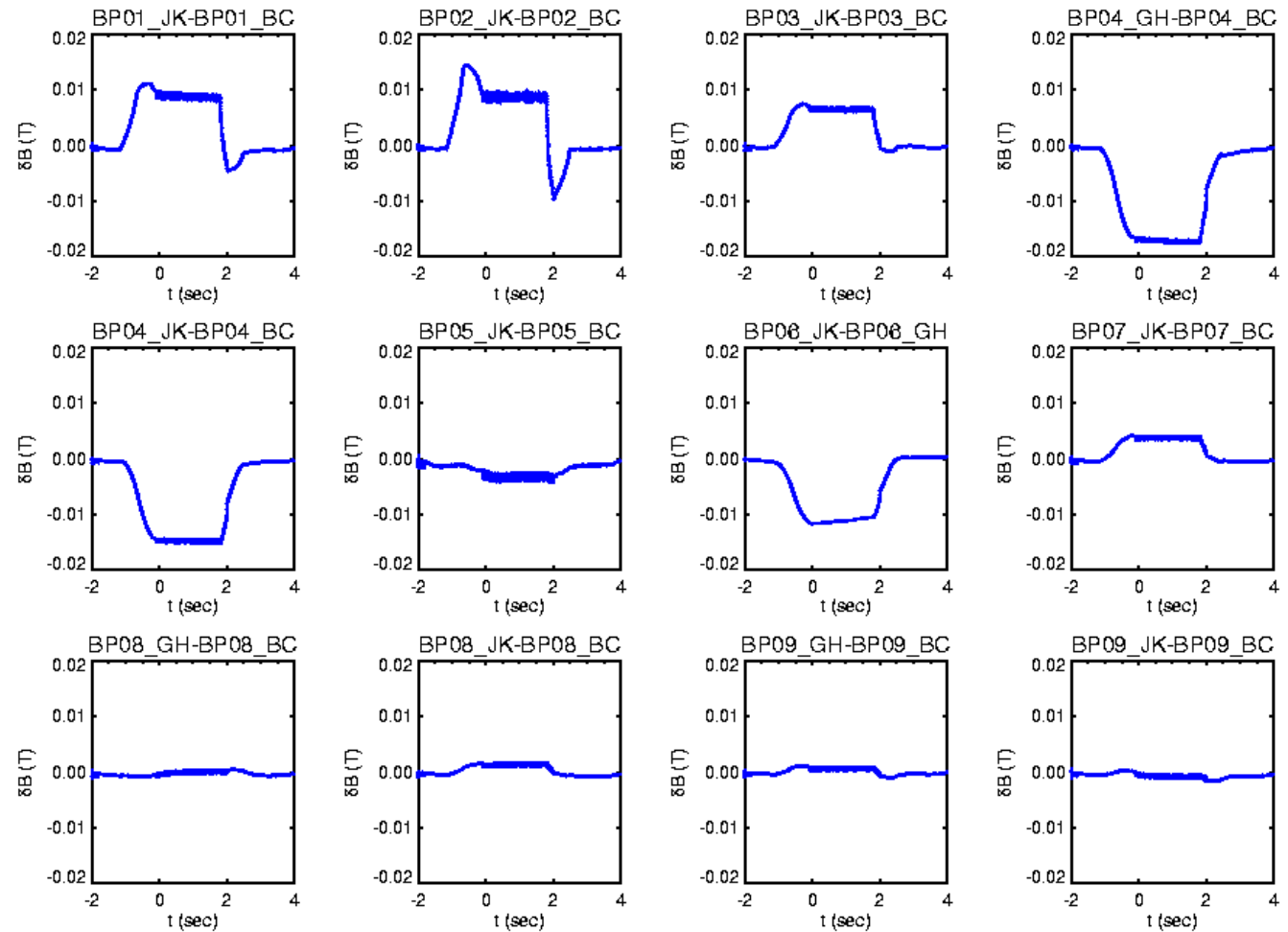
OH1 winding and TF bus  $m = 2$  contributions are a significant fraction of the experimentally deduced error, and are in the correct quadrant.

OH2 winding errors are substantial but happen to have non-resonant helicity (negative  $m$ ).

# Diagnostic Measurements and Coil Tests



### Difference Signals of BP loops Analyzed for Non-axisymmetric Fields



Individual  $B_p$  loops (total 77) at same poloidal locations, up to 4 toroidal locations, give differences indicating non-axisymmetry.

Each PF coil is powered separately in tests to determine their asymmetric contributions.

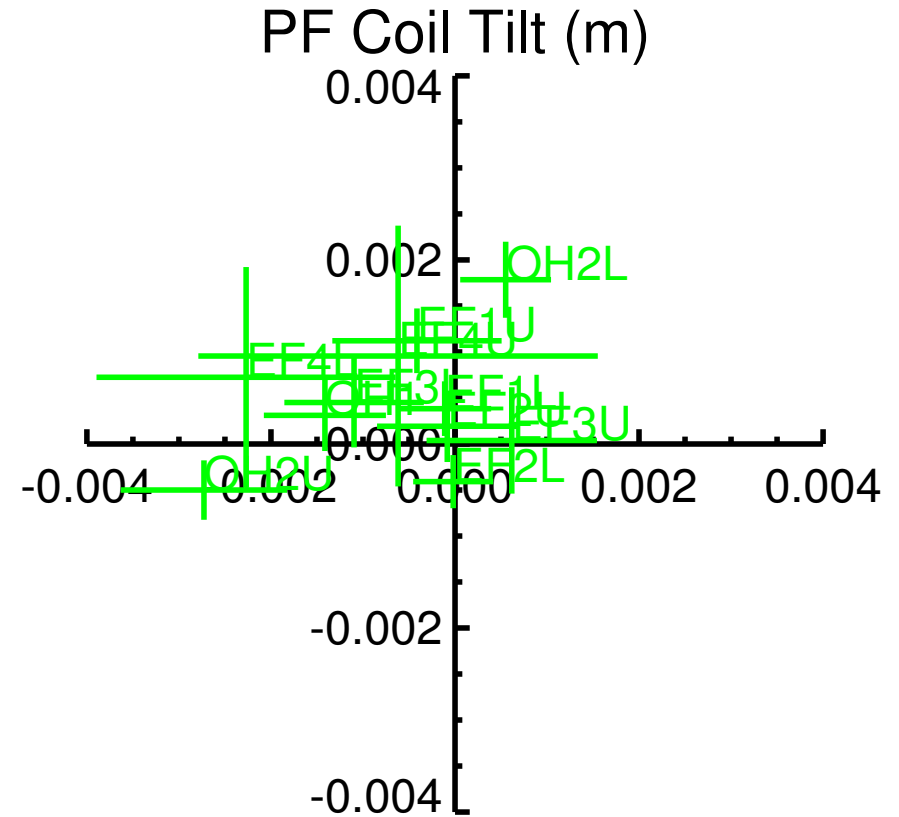
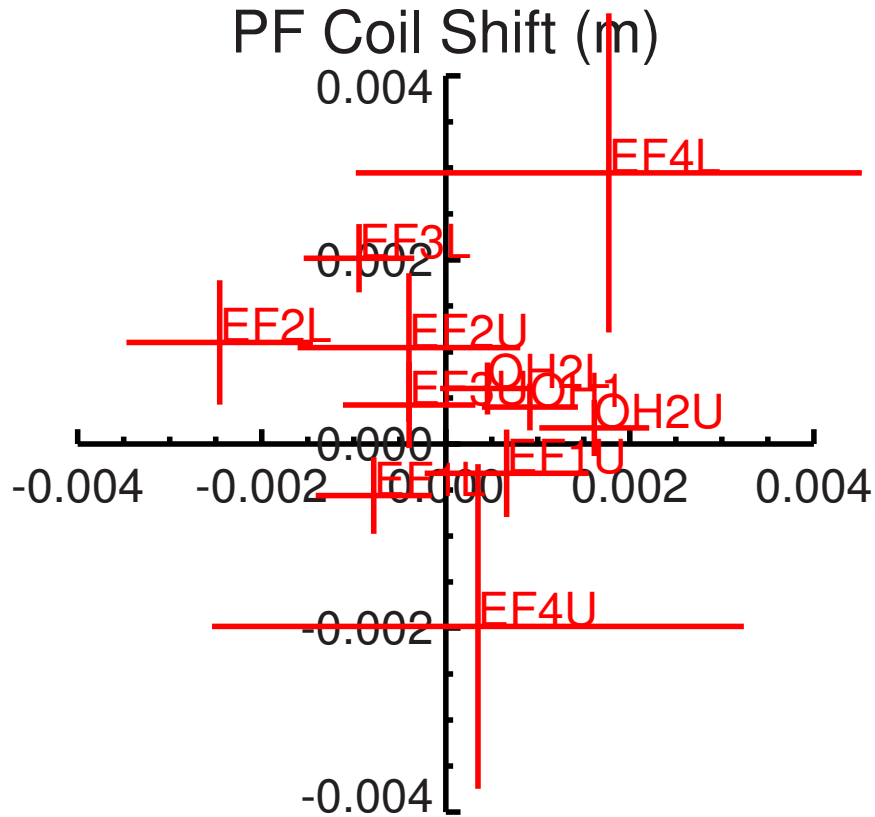
# Tests with individual coil currents fitted to deduce coil and measurement errors

Calculated known errors from OH winding and TF bus are subtracted. Remaining magnetic measurements are fitted using least squares with specified uncertainty:

Quantities	Number	Uncertainty Applied
<b>Measured Signals:</b>		
Field Differences ( $B_{pj} - B_{pi}$ )	13x51	.0005(T)+.002B <sub>p</sub>
Total	663	
<b>Parameters Fitted:</b>		
PF Coil Shifts and Tilts	4x11	.002 R
Measurement Parameters:		
Gain discrepancies	51	.01
Position	2x51	.001*R   , 0.0005*R ⊥
Poloidal Tilt	51	.017 (rad)
Total	248	

Reduced  $\chi^2 \sim 1$  is obtained, indicating consistency within errors.

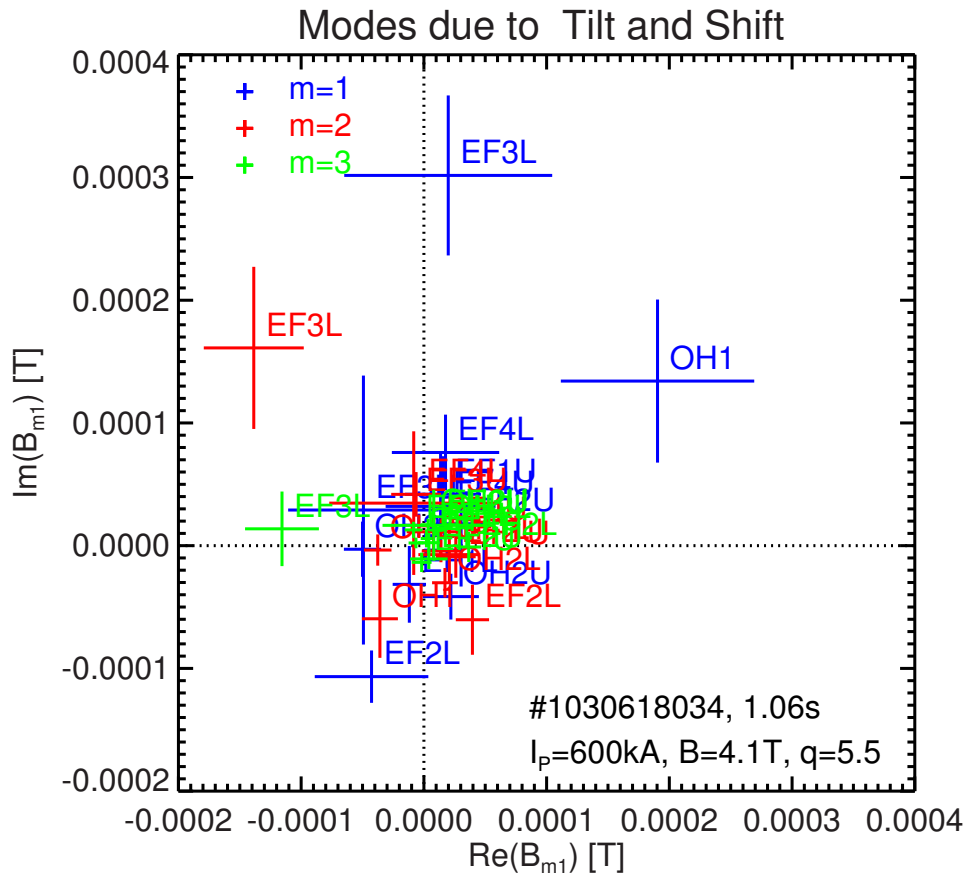
# Coil Shifts and Tilts deduced from fitting



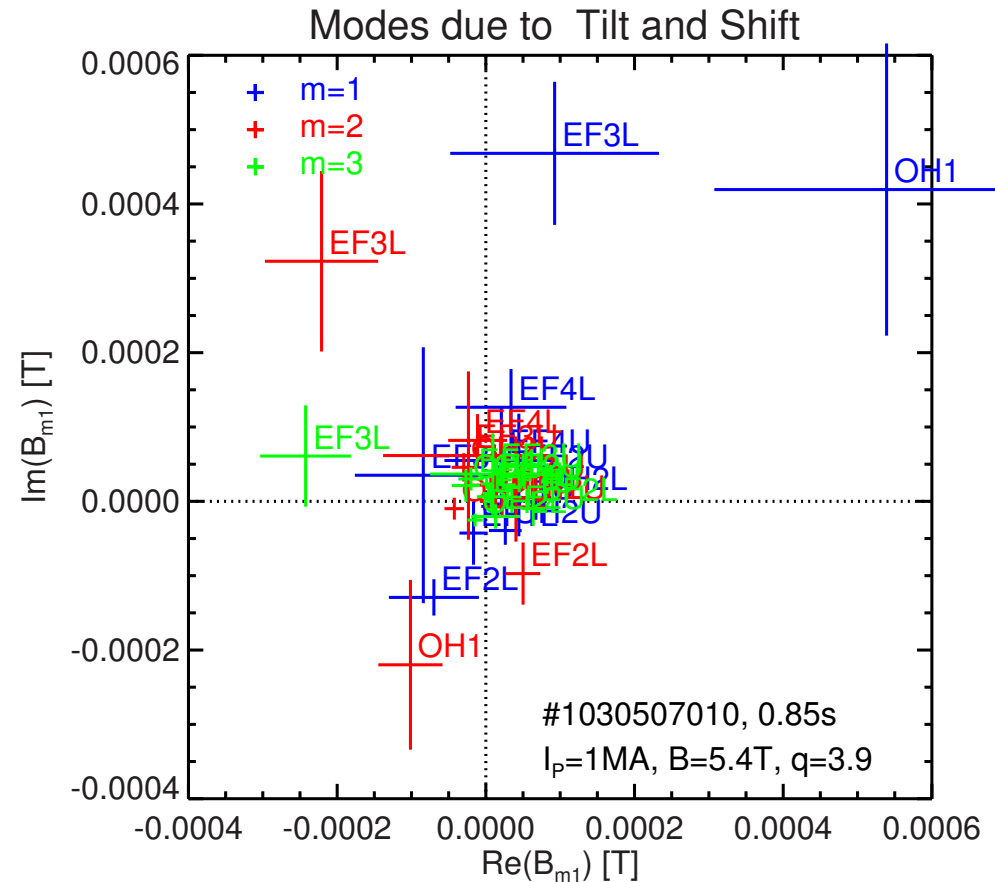
are of the order of a few millimeters.

Of course the fit constrains these to be small, but that we can get a low  $\chi^2$  result is a demonstration of at least consistency: Our test results are fitted with plausible tilts and shifts (plus known errors).

# Model's Tilts and Shifts give Significant Mode Contributions



Lower Plasma Current

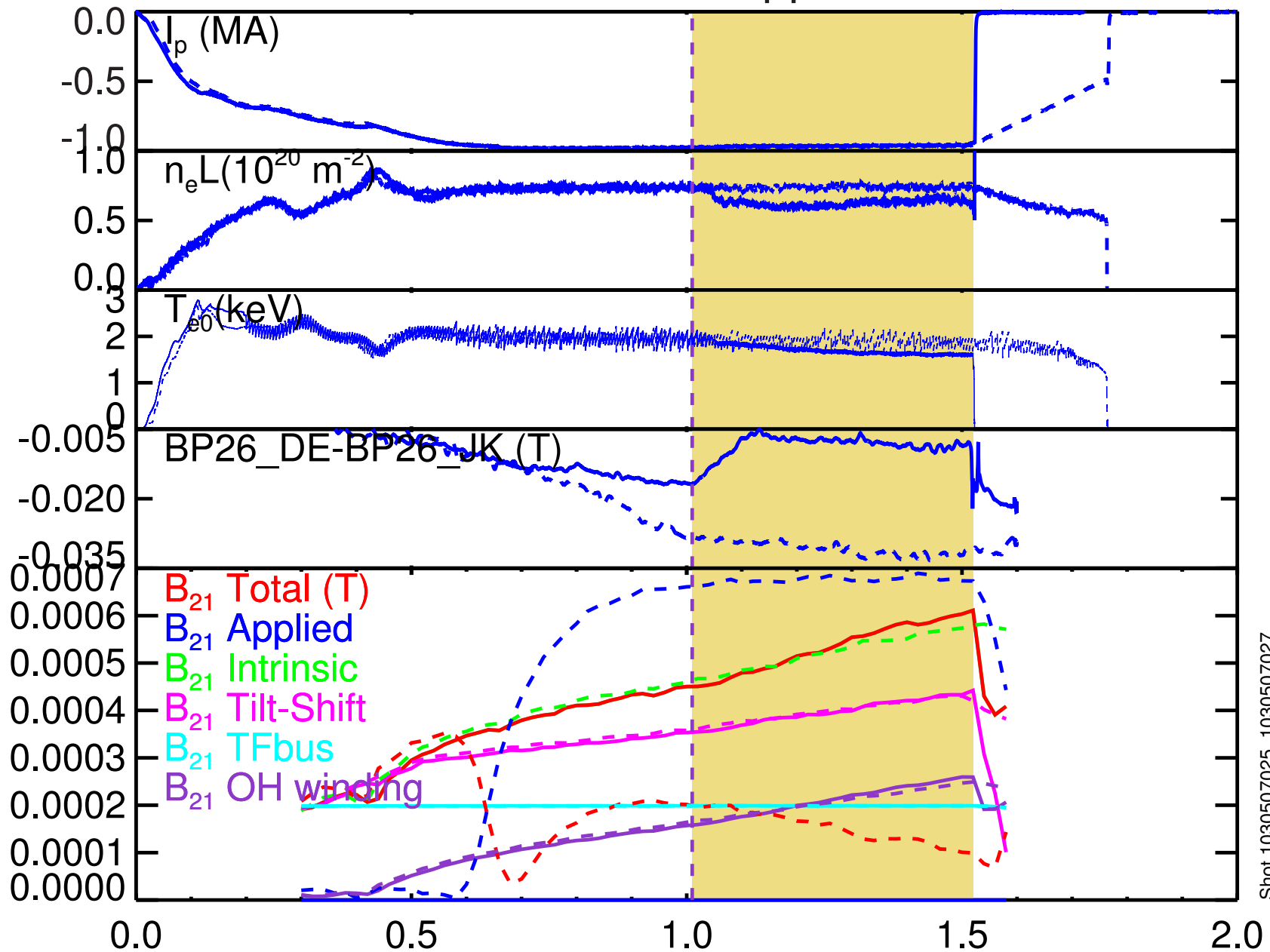


Higher Plasma Current

$m = 2$  (red) contributions are thought to be the most important.

Their sum is near the negative real axis, but varies with time as the flux swings.

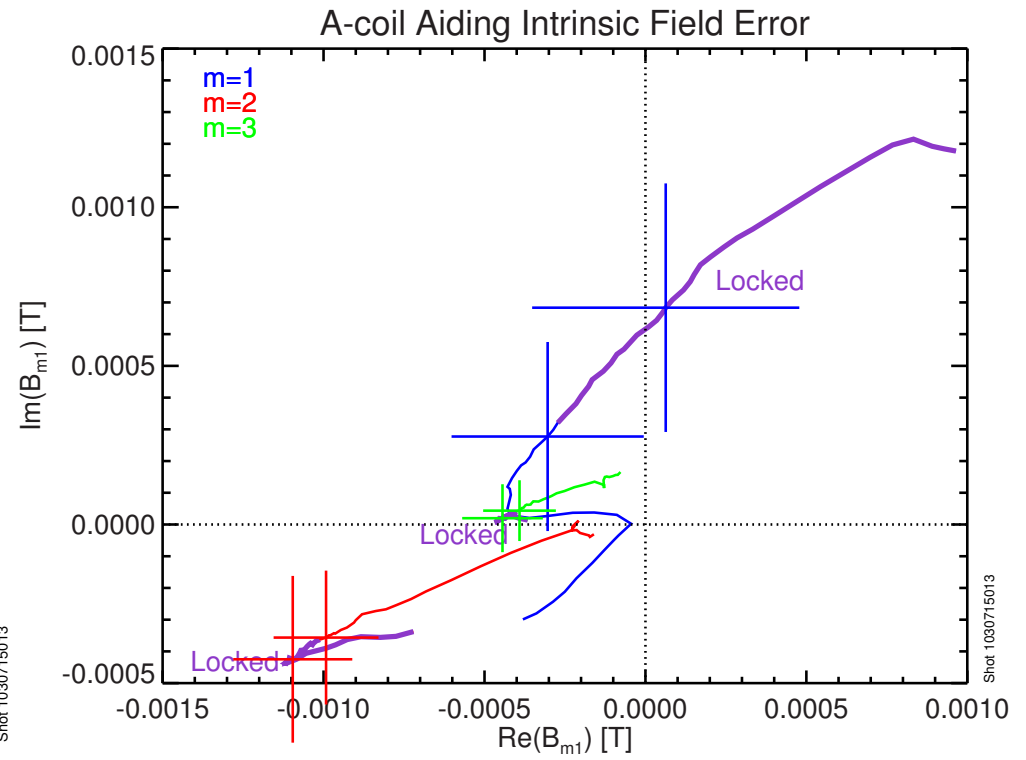
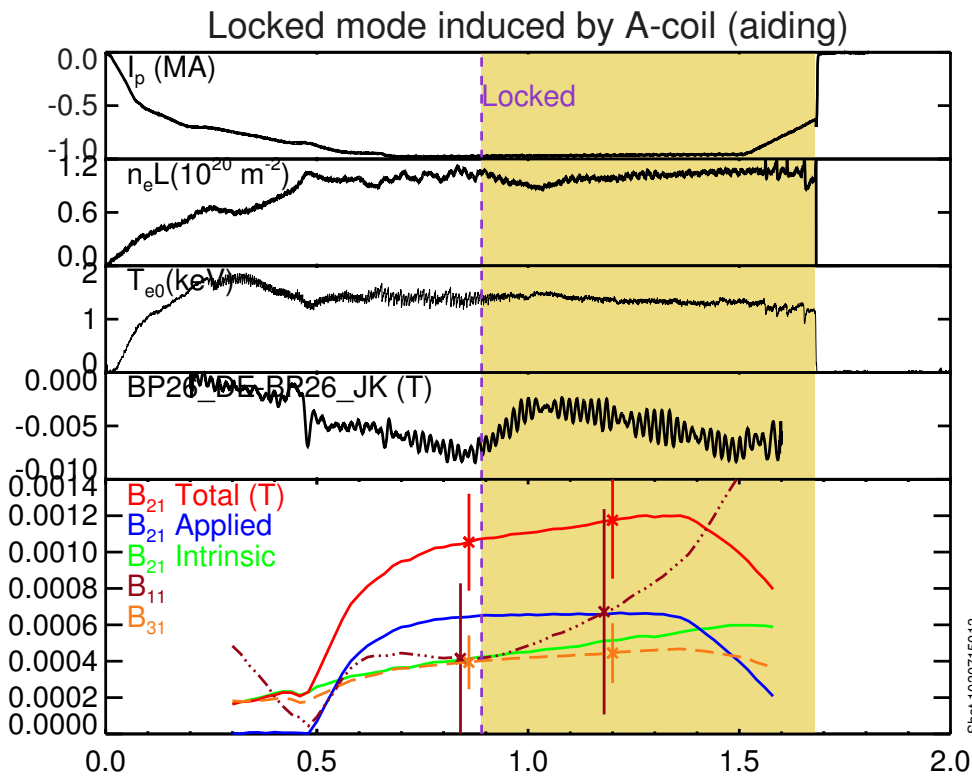
# Analysis into Applied and Intrinsic Model Components of Locked Mode Suppression



Shot 1030507025, 1030507027

(Solid lines: no applied field. Dashed lines: applied suppression.)

# Applied Field Reinforcing Intrinsic Field Locks at High density



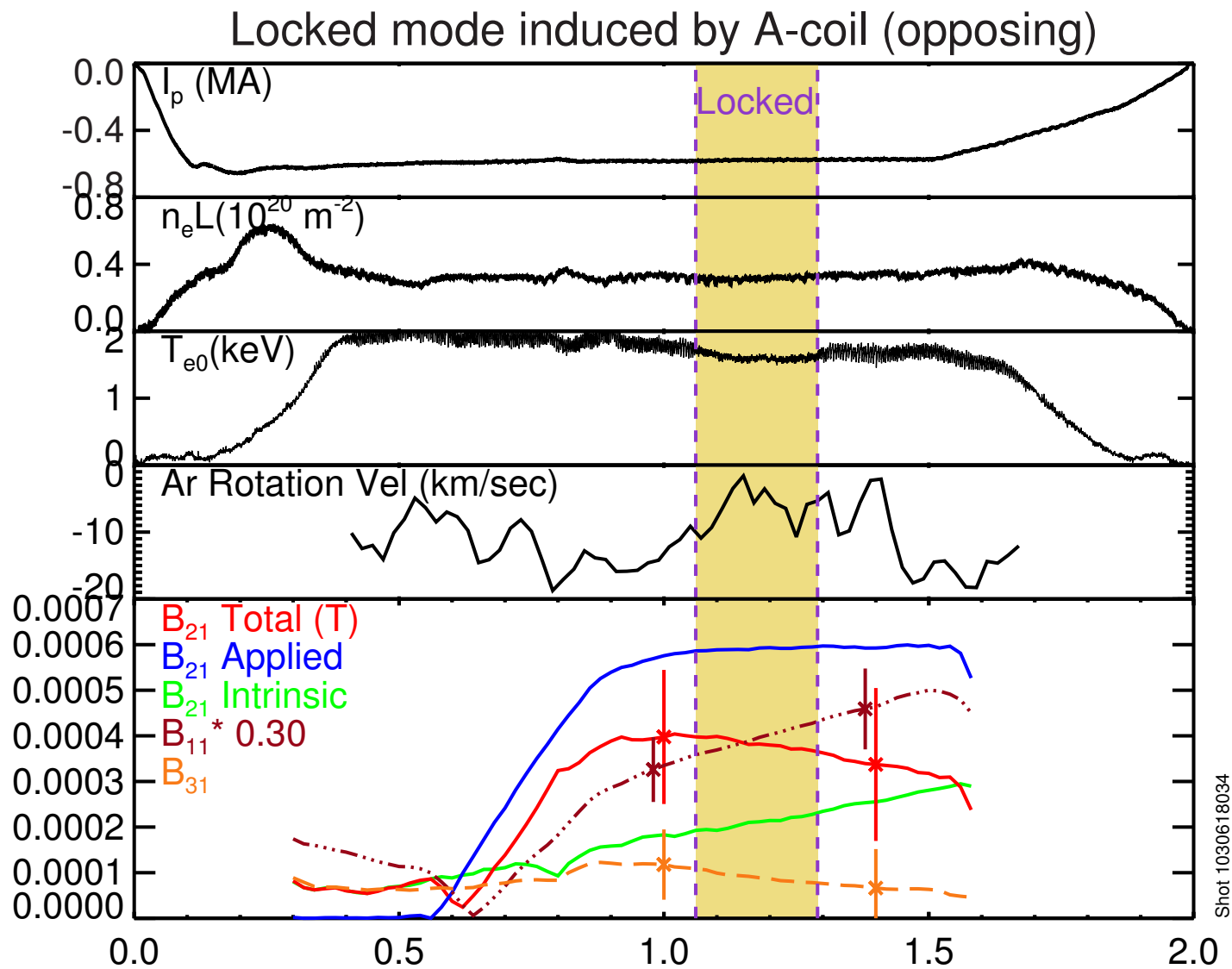
Upward drift of total  $B_{21}$  (red) caused by intrinsic field (green) evolution.

May explain the time delay for locking sometimes observed.

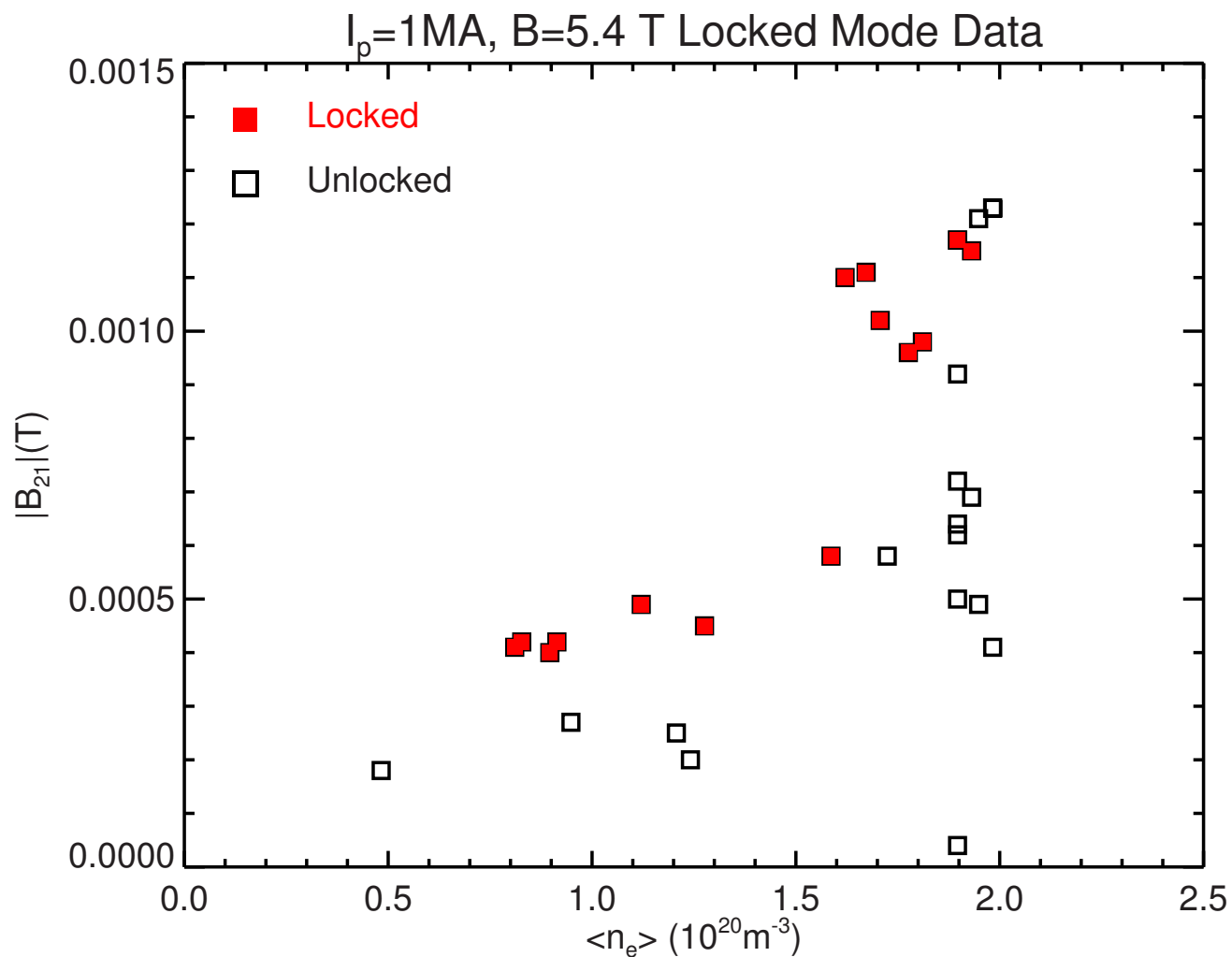
$B_{21}$  locking level  $\approx 1$  mT at this high density.

The  $B_{11}$  mode has large time variation, which seems to bear little relationship to locking.

# Locking/Unlocking Occurs slightly delayed from Total field maximum



# Database Analysis Is Just Beginning



Some suggestion of non-linear density scaling.

Requires additional data to verify.

Sideband analysis (not shown) indicates that  $m=1$  to  $m=2$  coupling may be significant.

# Conclusions

Newly installed A-coils valuable for locking control and rotation expts, generate or suppress locking, lowering locking density by factor 4.

C-Mod observed locked modes at up to  $\bar{n}_e = 1.9 \times 10^{20} \text{ m}^{-3}$

Experimentally determined intrinsic error field, e.g.  $\sim .35 \text{ mT @ } 0.6 \text{ MA}$ .

Designed-in field errors identified, OH+TF adding to as much as 0.5 mT, approximately in the experimentally deduced direction.

Fitting to PF coil tilt and shift indicates additional errors of comparable magnitude.

Model appears generally consistent with observations.

Locked mode data from C-Mod supports more optimistic scaling to ITER, not the strong size scaling deduced from Compass data.